Available online at www.sciencedirect.com
SCIENCE DIRECT
Journal of Sound and Vibration 293 (2006) 766–776
JOURNAL OF SOUND AND VIBRATION
www.elsevier.com/locate/jsvi

An investigation into the influence of longitudinal creepage on railway squeal noise due to lateral creepage

A.D. Monk-Steel[a,*], D.J. Thompson[a], F.G. de Beer[b], M.H.A. Janssens[b]

[a]*Institute of Sound and Vibration Research, University of Southampton, Highfield, Southampton SO17 1BJ, UK*
[b]*TNO TPD, Stieltjesweg 1, P.O. Box 155, 2600 AD Delft, The Netherlands*

Accepted 26 August 2005
Available online 24 January 2006

Abstract

Curve squeal noise is of growing concern for the railway industry as rail systems become more widespread in densely populated areas. In response to the pressure to minimise environmental pollution, there is a demand for a deeper understanding of the phenomenon and to develop a methodical approach to managing the wheel–rail system. Under curving, the wheel and the rail are subject to creep forces due to relative motion (creepage) within the contact region. In tight curves, these creep forces can cause unstable vibration of the wheel, leading to the radiation of squeal noise. The occurrence and characteristics of this are governed by the configuration of the creepages at the wheel–rail contact, which can have longitudinal, lateral and spin components. It follows that the representation of creepage is important in modelling the mechanisms of squeal noise behaviour. An investigation is presented into how the relationship between lateral creepage and creep force is affected when a component of longitudinal creepage is introduced. A 1:3 scale laboratory test rig has been modified to simulate contact conditions with controlled levels of lateral and longitudinal creepage, and to measure the salient system parameters. The experimental results are presented and discussed here.

1. Introduction

The dynamic behaviour of a railway vehicle in a section of curved track generates relative slip (creepage) at the wheel–rail interface in longitudinal, lateral and spin directions. In tight curves, high levels of creepage can develop into unstable stick/slip vibration, causing the wheels to radiate a loud, annoying sound known as curve squeal. Two main types of squeal noise have been identified: (i) stick/slip excitation due to lateral creepage of the wheel, and (ii) squeal due to contact on the wheel flange. Previous investigations into curve squeal noise have concentrated on squeal purely due to lateral creepage of the contact between the wheel tyre and the top of the crown of the rail [1–9]. Generally, this is because squeal noise is closely linked to the axial bending modes of a railway wheel, excited by contact forces acting in the lateral direction.

*Corresponding author. Tel.: +44 23 8059 3605; fax: +44 23 8059 3190.
E-mail addresses: ams@isvr.soton.ac.uk (A.D. Monk-Steel), djt@isvr.soton.ac.uk (D.J. Thompson).

0022-460X/$ - see front matter © 2006 Elsevier Ltd. All rights reserved.
doi:10.1016/j.jsv.2005.12.004

Rudd [1] proposed that instability in the lateral friction force acting on a wheel during curving is the dominant cause of squeal noise. He presented a simple model based on the relationship between creepage and creep force. It was used to determine the minimum effectiveness of a damping treatment applied to a wheel to suppress squeal by equating it to the shortfall between the force input due to stick/slip and the losses due to internal damping of the wheel and its acoustic radiation. The creep characteristic used by Rudd was based on data obtained from experiments on a rolling rig. Compared with other models, this characteristic has been found to show an excessive decline in creep force as the creepage grows beyond saturation. As a result, the model tends to over-estimate the minimum level of damping required to suppress squeal (see also Ref. [2]). However, Rudd's work demonstrated the importance of the relationship between friction and creepage in squeal behaviour, and many subsequent models adopt parts of Rudd's approach in the theoretical modelling of railway curve squeal.

Fingberg [3,4] and Périard [5] have expanded this basic model by including improved models of wheel dynamics, friction characteristics and the sound radiation of the wheel. They incorporated different empirical models of sliding friction between a wheel and a rail to describe the decrease in creep force with increasing creepage.

de Beer et al. [6,7] presented a similar theoretical model based on excitation by unstable lateral creepage. They have also developed an experimental rig based on a reduced scale wheel and a roller representing the rail [8,9]. Squeal behaviour in rolling contact could be replicated by imposing a yaw angle between the wheel and the rail roller. Furthermore, measurements on the rig supported findings from the theoretical study that instability in the squeal noise mechanism was dependent on the lateral position of contact on the wheel tyre. Unstable stick/slip motion was associated with the offset of contact from the normal running position away from the flange. This is normally seen at the leading inner wheel of a bogie or two-axle vehicle in a curve. Stable motion was associated with the conditions of the leading outer wheel where, conversely, contact on the wheel shifts laterally towards the flange.

During curving the leading wheelset of a bogie tends to move outwards into flange contact on the outer wheel. Due to its yaw angle with the rail, the inner wheel experiences large lateral creepage, leading to a force acting outwards on the wheel, whereas the flange contact on the outer wheel leads to a restoring force acting inwards [10]. The typical forces acting on the wheels of a bogie are shown schematically in Fig. 1. From this it will be seen that, as well as the lateral creep forces, longitudinal creep forces also act.

Lateral creepage is thus likely to exist in combination with longitudinal creepage and the influence of longitudinal creepage on the mechanism of squeal noise behaviour, specifically the creepage/creep force relationship, is of interest. This paper presents some experimental results obtained for combined longitudinal and lateral creepage. The rig of de Beer et al. has been adapted to investigate the relationship between creepage and creep forces in the presence of longitudinal creepage. Some of the results from this investigation are presented and discussed.

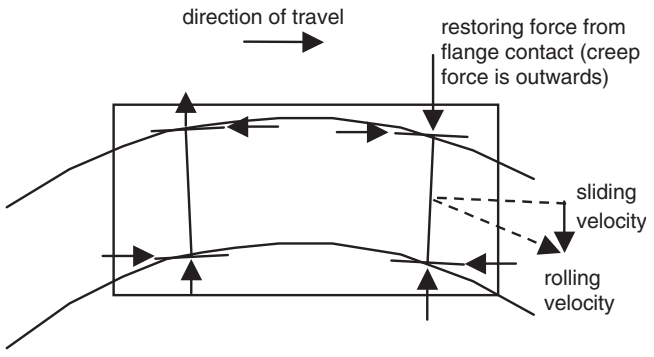

Fig. 1. Schematic view of forces acting on the wheels of a bogie in a curve.

2. Creepage and creep force

2.1. The relationship between creep force and creepage

When a wheel rolls on the rail, relative motion can occur between the wheel and the rail at their contact. The creepage is defined as the relative velocity divided by the rolling velocity. Thus, in the longitudinal direction, it is given by $\gamma_1 = v_1/V$, where $v_1 = v_1^W - v_1^R$ is the relative velocity and V is the rolling velocity. The relationship between creep force and creepage for two elastic bodies in rolling contact has been found to have a characteristic resembling that shown in Fig. 2. The plot relates positive values of creepage to negative values of creep force because the force acts in the opposite direction to the relative motion.

Where the tangential forces are small, the elasticity of the wheel and rail materials allows the contact patch to be made up of a large area, where the surfaces are locked together in adhesion, and a small area at the trailing edge, where there is relative motion. Creep force and creepage are related linearly in this regime. As the creep force increases, the area in adhesion reduces and the area under slip increases. The creep force rises to reach a maximum level and is said to have reached *saturation* when the entire contact region is under slip. With increasing sliding velocity, the dynamic friction coefficient decreases. It is this characteristic that allows the unstable vibration to develop, leading to squeal noise behaviour. Various models for the relationship between creep force and creepage are outlined below.

2.2. Modelling the linear regime

The theory of rolling contact has been developed by Kalker [11]. His linear theory describes the relationship between creep force and creepage between two bodies in rolling contact at low levels of creepage. In the case of longitudinal creepage, the creep force F_1 increases linearly in proportion to the longitudinal creepage γ_1:

$$F_1 = -GabC_{11}\gamma_1, \tag{1}$$

where G is the shear modulus (assuming that the rail and wheel materials are identical), a and b are the contact patch semi-axis lengths, assuming the contact patch to be an ellipse (a is in the direction of rolling). The creep coefficient C_{11} depends on the Poisson's ratio of the wheel and rail material(s) and on the aspect ratio a/b. Kalker determined these coefficients and presented them in a table. The minus sign indicates that the creep force acts in the opposite direction to the creepage. Note that Eq. (1) is independent of the friction coefficient.

Creepage in the lateral direction, $\gamma_2 = v_2/V$, produces a corresponding lateral creep force F_2. However, when the contact patch is inclined relative to the axis of rotation, a relative rotational velocity Ω_3 about the axis perpendicular to the contact plane exists. The corresponding spin creepage is defined as $\omega_3 = \Omega_3/V$ (rad/m). For a contact angle ϕ between the plane of the contact and the axis of rotation, the spin creepage is given by

$$\omega_3 = \frac{\sin\phi}{r_0}, \tag{2}$$

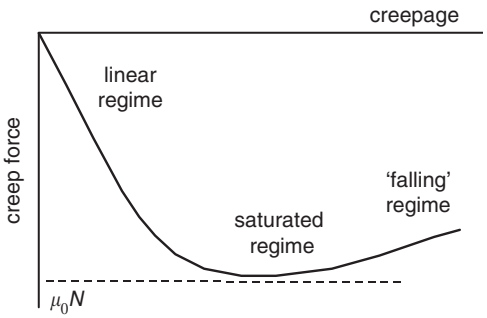

Fig. 2. Shape and regimes associated with a plot describing the relationship between creep force and creepage.

with r_0 the wheel radius. Spin creepage is generally only significant in the case of flange contact, where the contact angle can be very large. Both lateral and spin creepages generate a lateral force and a spin moment at the contact. At low values of creepage, linear theory gives these as

$$F_2 = -GabC_{22}\gamma_2 - G(ab)^{3/2}C_{23}\omega_3, \tag{3}$$

$$M_3 = G(ab)^{3/2}C_{23}\gamma_2 - G(ab)^2C_{33}\omega_3, \tag{4}$$

where C_{22}, C_{23} and C_{33} are creep coefficients, also tabulated by Kalker [11].

2.3. Modelling the saturation of creep force

As creep force increases it cannot exceed μN, where μ is the coefficient of friction and N is the normal load. Kalker [11] gives detailed theory for nonlinear creep, which requires numerical solution. However, an approximation for this saturation of creep is given by Shen et al. [12]:

$$F_i = \begin{cases} -\mu_0 N(\Gamma_i - \frac{1}{3}\Gamma_i^2 + \frac{1}{27}\Gamma_i^3) & \text{for } \Gamma_i < 3, \\ -\mu_0 N & \text{for } \Gamma_i > 3, \end{cases} \tag{5}$$

where F_i is the longitudinal or lateral creep force and Γ_i is a normalised creep given by

$$\Gamma_i = \frac{GC_{ii}ab}{\mu_0 N}\gamma_i \quad \text{for } i = 1, 2. \tag{6}$$

At very low creepages, the above equation approximates Kalker's linear theory. As creepage increases towards the saturation of creep force, a cubic function is used to limit the creep force to $\mu_0 N$. For creepages beyond saturation, the creep force is assumed to remain at this level because the model does not account for the falling regime.

2.4. Combined lateral and longitudinal creepage

Hedrick and Wormley [13] extended the above model to give a so-called heuristic model to allow for the combination of lateral and longitudinal creepage. The resultant of the *linear* lateral and longitudinal creep forces, F_s, neglecting the spin moment M_3 (which is small in comparison to other moments on the wheelset) is given by

$$F_s = (F_1^2 + F_2^2)^{1/2}, \tag{7}$$

where F_1 and F_2 are given by Eqs. (1) and (3). The linear force is reduced to the nonlinear value according to the following law:

$$F_s' = \left[\frac{F_s}{\mu N} - \frac{1}{3}\left(\frac{F_s}{\mu N}\right)^2 + \frac{1}{27}\left(\frac{F_s}{\mu N}\right)^3\right]\mu N \quad \text{for } F_s \leqslant 3\mu N, \tag{8}$$

$$F_s' = \mu N \quad \text{for } F_s \geqslant 3\mu N. \tag{9}$$

A reduction coefficient ε is then defined as

$$\varepsilon = \frac{F_s'}{F_s}, \tag{10}$$

and the nonlinear longitudinal and lateral creep forces are given by

$$F_1' = F_1\varepsilon, \quad F_2' = F_2\varepsilon. \tag{11}$$

2.5. Modelling the falling regime

In the falling regime, the coefficient of friction μ_0 falls as the sliding velocity increases. Fingberg [4] and de Beer [6] used the semi-analytical expression given by Kraft [14]:

$$\mu_0(v) = \mu_{\text{stat}}\{1 - 0.5\text{e}^{-0.138/|v|} - 0.5\text{e}^{-6.9/|v|}\}, \tag{12}$$

where μ_{stat} is the static coefficient of friction. The sliding velocity v can be expressed as $v = \gamma V$, where γ is either the lateral or longitudinal creepage (or a combination) and V is the rolling velocity. The first exponential term in Eq. (12) causes a rapid drop in the friction coefficient for small sliding velocities, whereas the second exponential term ensures a further reduction at higher sliding velocities.

Périard [5] used two empirical friction laws obtained from an overview by Kragelski [15]. Both were based on measurements of a sliding railway wheel. Poiré and Bochet's study of a wheel sliding on a rail for speeds up to 20 m/s gave the friction coefficient as

$$\mu_0(v) = \mu_{\text{stat}}\left\{\frac{1}{1 + 0.03|v|}\right\}, \tag{13}$$

where typical values for μ_{stat} are given as 0.31 for a very dry rail, 0.22 for a dry rail and 0.14 for a wet rail [5]. Galton investigated the sliding contact of a wheel and a brake block, and presented the following model, derived from the experimental results. This may not be applicable in the case of curve squeal as the contact conditions between and wheel and brake block are not necessarily comparable with those at the wheel–rail interface under curving:

$$\mu_0(v) = \mu_{\text{stat}}\left\{\frac{1 + 0.018|v|}{1 + 0.097|v|}\right\}, \tag{14}$$

with typical values for μ_{stat} given as 0.45 for dry conditions and 0.25 for moist surfaces [5].

Remington [2] presents measurements of the coefficient of friction measured on a twin disc roller rig. This consisted of a 190-mm diameter wheel and 760-mm diameter 'rail-wheel'. These results were compared with a model given by Rudd [1] with suitably chosen parameter values. Reasonable agreement with the measured data points was found. Rudd's model represents the adhesion coefficient μ (creep force divided by normal load) as

$$\mu = \mu_0 \frac{\gamma}{\gamma_0} \exp\left(1 - \frac{\gamma}{\gamma_0}\right), \tag{15}$$

where μ_0 and γ_0 are constants (chosen as 0.4 and 0.009, respectively, in Ref. [2]) and γ is the creepage. Note that μ_0 is the maximum value of the curve, not necessarily the static friction coefficient. This model was chosen 'to get a feel for' the excitation of squeal, and is given as 'the simplest analytical expression with ... the form' that μ is proportional to γ at small values of creepage, reaches a maximum and then decreases [1].

The results from the various models are compared in Fig. 3, for a value of $\mu_{\text{stat}} = 0.4$ (for Rudd's model $\mu_0 = 0.4$). Since the equations of Kraft, Poiré and Galton are based on a sliding velocity and that of Rudd is based on a creepage, a value has to be assumed for the rolling velocity to allow direct comparison. Here 10 m/s is used. It is clear that Kraft gives a friction characteristic with a much steeper slope than Poiré or Galton, but considerably less steep than Rudd.

3. Test rig

A reduced scale rolling rig has previously been developed to simulate and observe a range of contact conditions associated with wheel–rail contact in curved track and to investigate squeal behaviour caused by lateral creepage [6–9]. Typical contact conditions between a mainline railway wheel and rail are represented using a pair of steel wheels that are approximately one-third of the full size. Both wheels have a radius of 0.125 m. The lower wheel, the 'rail-roller', is damped by a series of thin plates bolted to the web. It is connected to an electric motor of variable rotational speed. The upper wheel is supported in contact with the rail-roller

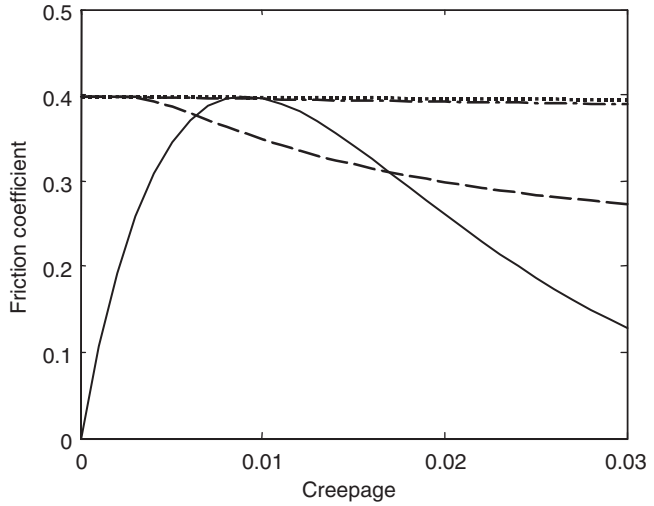

Fig. 3. Comparison of friction or adhesion coefficients from different models of a wheel on a rail for a rolling velocity of 10 m/s. —— rolling friction according to Rudd, – – – sliding friction according to Kraft, ····· sliding friction according to Poiré/Bochet, – · – according to Galton. In each case $\mu_{stat} = 0.4$ (for Rudd's model $\mu_0 = 0.4$).

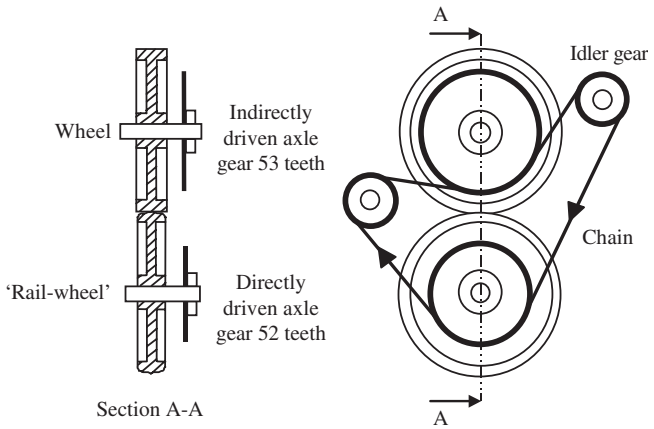

Fig. 4. Schematic view of the chain and gear wheel transmission to create a fixed longitudinal creepage of 2%.

within a structure that allows variation in the lateral offset of contact on the wheel tyre, the rolling (yaw) angle, and the contact load.

For the present investigation, the rig has been modified so that it can also introduce controlled levels of longitudinal creepage. This is achieved by imposing a relative velocity in the contact region by controlling the individual rolling velocities and rolling radii of the wheel and the 'rail-roller'. The method is based on the transmission of rotation between the shafts of the two wheels using an arrangement of toothed gears linked by a chain. A schematic view is shown in Fig. 4. To obtain variation in the level of longitudinal creepage, a mismatch in the number of teeth on the main gears is used, while the rolling radii of the 'wheel' and 'rail-roller' are equal.

For the present investigation, the rig was used to observe how the relationship between lateral creepage and creep force is modified if a fixed component of longitudinal creepage is introduced. The gear ratio indicated in Fig. 4 was used to generate a fixed longitudinal creepage of 2%. Additional variations in longitudinal creepage can be introduced by using tapered wheels.

4. Results

A series of tests was performed to give variation in the level of lateral creepage for two contact positions on the wheel tyre. One position was chosen such that squeal occurred ('unstable position'), while, at the other, the contact position was such that squeal did not occur [6]. A range of yaw angles was used up to 2.5°, with 1° (or 17 mrad) corresponding to 1.7% lateral creepage. The normal load was 1 kN and the wheel rotation speed was 90 rev/min or 1.2 m/s. These tests were performed before and after the rig was modified and the results are compared in Figs. 5 and 6 to evaluate the repeatability of the rig and test methods. Before each measurement, the wheel tyres were cleaned using sandpaper and acetone. Before each measurement was taken, a short time was allowed for the contact conditions to stabilise; debris due to wear and acetone each act like a lubricant and

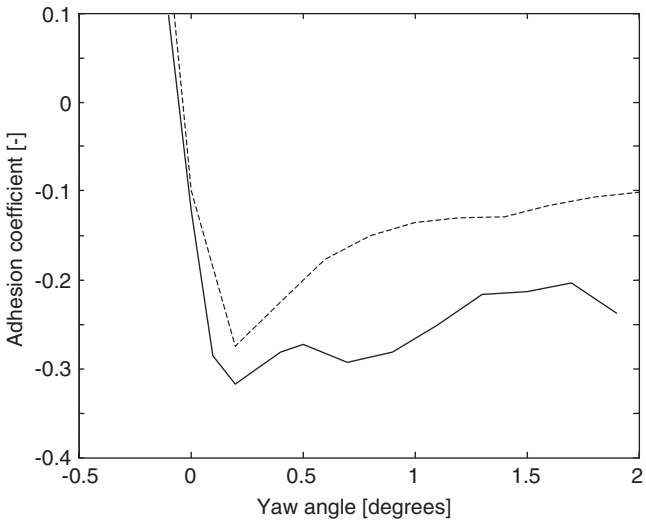

Fig. 5. Measured relationship between the lateral adhesion coefficient and lateral creepage in the unstable contact position. — measured at the beginning of the tests; – – – measured at the end of the tests.

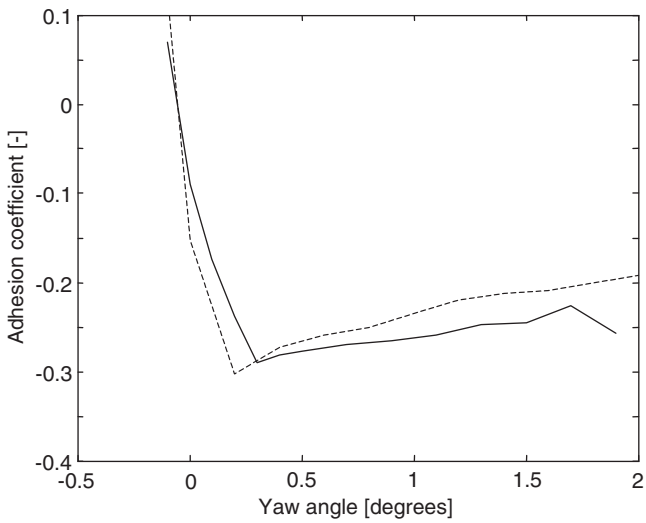

Fig. 6. Measured relationship between the lateral adhesion coefficient and lateral creepage in the stable contact position. — measured at the beginning of the tests; – – – measured at the end of the tests.

so must be avoided. The frictional conditions of the running surfaces were assessed by determining the relationship between lateral creep force and lateral creepage over a number of short, successive tests. The contact conditions were considered to have stabilised once the creep force at saturation had reached a maximum and a repeatable creep characteristic could be produced with a corresponding occurrence of squeal noise. Nevertheless, the results are subject to measurement errors due to the limited accuracy of the test rig and the difficulty to control all the parameters during the measurement.

Measurements of lateral creep force with variation in lateral creepage were carried out with the chain in place to impose a 2% longitudinal creepage. The range of yaw angles available was limited when using the chain, due to excessive misalignment of the gears. The resulting friction characteristics are shown in Figs. 7 and 8. In the unstable contact position and with no longitudinal creepage, continuous squeal noise was

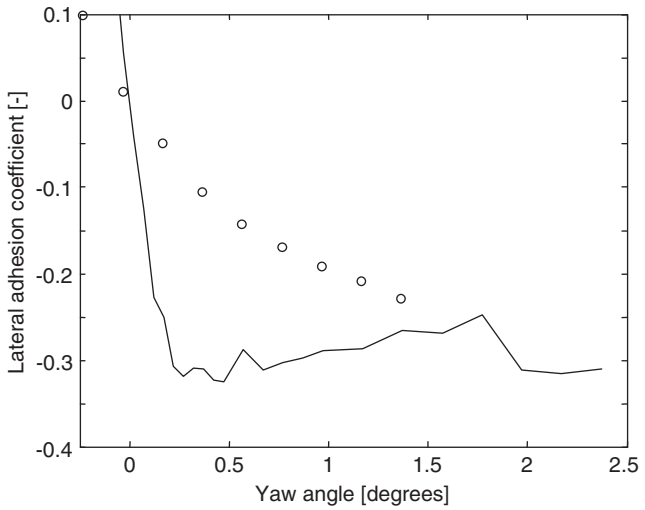

Fig. 7. Measured relationship between the lateral adhesion coefficient and lateral creepage in the stable contact position. — lateral creepage only, no audible squeal behaviour; ○ combined longitudinal and lateral creepage, no audible squeal behaviour.

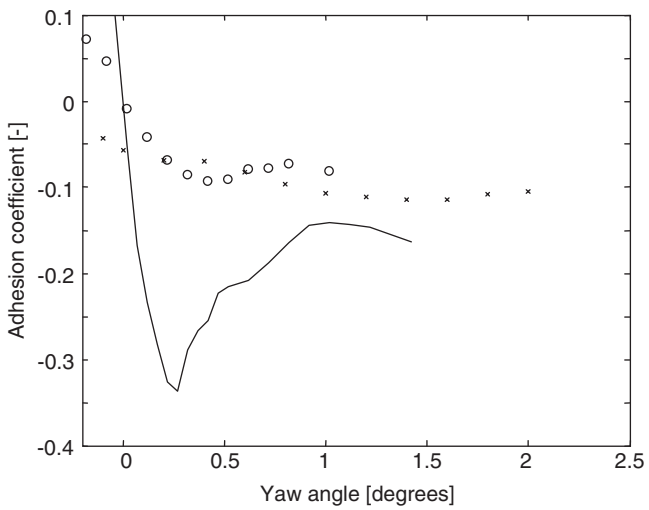

Fig. 8. Measured relationship between the lateral adhesion coefficient and lateral creepage in the unstable contact position. — lateral creepage only, no audible squeal behaviour; ○ first measurement of combined longitudinal and lateral creepage, no audible squeal behaviour; × second measurement with audible squeal behaviour at yaw angles of 1.4° and above.

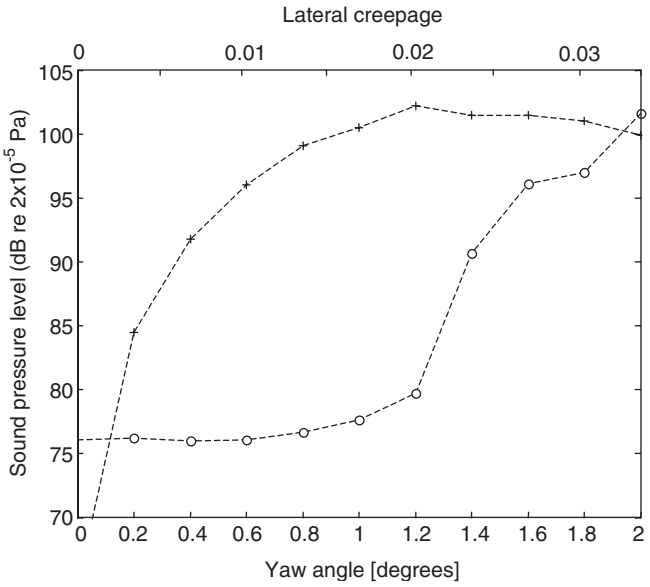

Fig. 9. Measured sound pressure level in the 1250 Hz one-third octave band at 0.5 m from the web of the wheel roller; - - + - - lateral creepage only; - - ○ - - with $\gamma_1 = 0.02$.

produced for yaw angles of 0.3° and above. With the chain attached to introduce 2% longitudinal creepage, initially no audible squeal noise was produced except with a yaw angle of around 1°, where squeal could be intermittently excited. It was noticed that if the chain came loose during the test then the wheel would immediately produce squeal, provided the minimum yaw angle of 0.3° was imposed. These results show that the presence of longitudinal creepage reduces the level of lateral creep force. It also changes the shape of the curve, so that it does not develop the falling regime at the higher values of yaw angle seen in the absence of longitudinal creepage.

A second test in the unstable contact position was performed in order to obtain a noise measurement with and without longitudinal creepage present. Measurements were possible up to a yaw angle of 2°. It was found that continuous audible squeal noise is radiated in the case with longitudinal creepage when higher yaw angles are reached. The sound pressure level at 0.5 m from the web of the wheel was measured. The results are given in Fig. 9 and compared with an equivalent noise measurement in the case of lateral creepage alone. In both cases, squeal noise made by the wheel is dominated by a tone in the 1250 Hz one-third octave frequency band. The sound pressure level in this band at each yaw angle is plotted. This shows that in the presence of longitudinal creepage the onset of squeal noise occurs at higher levels of lateral creepage, commencing at yaw angles of 1.4°, whereas without longitudinal creepage squeal occurs from yaw angles of 0.4°. A yaw angle of 1.4° corresponds to a lateral creepage of 2.4%, which just exceeds the level of longitudinal creepage (2%).

The theoretical and measured adhesion coefficient curves for pure lateral creepage in the stable contact position are compared in Fig. 10. The theoretical curve is calculated using the values $N = 1.29$ kN, $a = 0.98$ mm, $b = 1.11$ mm, from which $C_{11} = 4.22$ and $C_{22} = 3.58$ are found. There is reasonable agreement if the coefficient of static friction μ_{stat} is chosen so that the creep force saturates as in the measurement. In order to give a better fit to the falling part of the curve, the first exponential term in Eq. (12) has been changed to give $\mu_0(v) = \mu_{\text{stat}}\{1 - 0.5\text{e}^{-0.05/|v|} - 0.5\text{e}^{-6.9/|v|}\}$. Also shown in the figure is a prediction for the case with 2% longitudinal creepage, based on Eqs. (7)–(11). This shows a good fit to the measurements. At this level of longitudinal creepage, the lateral creep force does not reduce with increasing yaw angle until angles greater than about 3°, where it reduces with a shallower slope than for pure lateral creep.

The creep force results for the unstable position cannot be reproduced using the models described here. The relation between quasi-static force and yaw angle is affected by the presence of stick-slip in the contact region, so that the mean slip velocity should include this as well as the steady creepage. In Ref. [6], an attempt was made to predict the effect for pure lateral creepage using the squeal noise model.

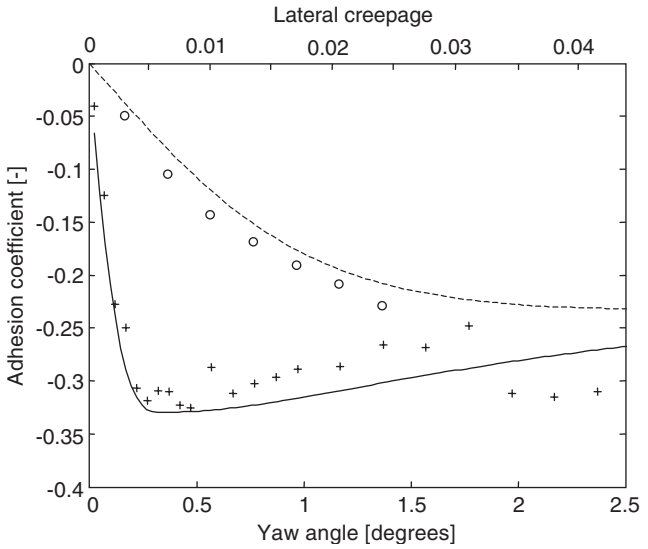

Fig. 10. Lateral adhesion coefficient and lateral creepage in the stable contact position. + measured, − predicted, for no longitudinal creepage; – – – measured, ○ predicted, with $\gamma_1 = 0.02$. μ_{stat} taken as 0.33.

5. Conclusions

Measurements were performed on a scaled rolling rig to observe how the relationship between lateral creepage and lateral adhesion coefficient is modified when a longitudinal creepage of 2% is imposed. It was found that for the same level of lateral creepage, the adhesion coefficient was significantly lower in the presence of longitudinal creepage. A sustained falling regime was not seen in the lateral friction force. Furthermore, continuous squeal noise was not audible during tests with this level of longitudinal creepage, except at higher yaw angles when the level of lateral creepage exceeds the longitudinal creepage. The saturation of tangential forces by longitudinal creepage may have suppressed the stick/slip mechanism in this case. In practice, the intermittent nature of curve squeal may be linked to the changing components of lateral and longitudinal creepages as a railway vehicle travels around a curve, as well as fluctuations in the friction coefficient of the running surfaces.

For a wheel in a curve, lateral creepage usually occurs in the presence of some longitudinal creepage, although the level of longitudinal creepage studied here is somewhat larger than would normally be present for the yaw angles considered. Further investigations will look more closely at contact conditions with varying levels of longitudinal creepage. To achieve a finer resolution, the relative velocity can be introduced by using a wheel with a tapered tread profile. Again, the chain and gear transmission can be used to impose a base level of creepage, which can be zero if the number of teeth on each of the gears is the same.

It is clear that a reliable model of curve squeal noise must take into account the presence of longitudinal creepage in addition to the lateral creepage usually considered to be the source of unstable vibration. The fact that the average lateral creep force reduces in the presence of squeal should also be considered in vehicle dynamics calculations.

The findings of this study suggest that railway curve squeal noise due to lateral creepage can be limited by imposing or allowing the development of longitudinal creepage at the wheel–rail interface. Practical applications of this may include, for example, the design of wheel and rail profiles, or the control of the dynamic behaviour of the railway vehicle through track or vehicle design.

Acknowledgements

The work described here was carried out within ‘Project A3—Railway noise: curve squeal, roughness growth, friction and wear’ for the EPSRC centre Rail Research UK. The authors are grateful to the Royal

Academy of Engineering, who supported the experimental work through a Global Research Award enabling the first author to spend 6 months at TNO TPD, Delft, the Netherlands.

References

[1] M.J. Rudd, Wheel/rail noise—part II: wheel squeal, *Journal of Sound and Vibration* 46 (1976) 381–394.
[2] P.J. Remington, Wheel/rail squeal and impact noise: What do we know? What don't we know? Where do we go from here?, *Journal of Sound and Vibration* 116 (1987) 339–353.
[3] U. Fingberg, A model for wheel-rail squealing noise, *Journal of Sound and Vibration* 143 (1990) 365–377.
[4] U. Finberg, Ein model für das Kurvenquietschen von Schienenfahrzeugen, Fortschritt-Berichte VDI, 1990, Reihe 11, No. 140.
[5] F. Périard, Wheel-Rail Noise Generation: Curve Squealing by Trams, PhD Thesis, Technische Universiteit Delft, 1998.
[6] F.G. de Beer, M.H.A. Janssens, P.P. Kooijman, Squeal noise of rail-bound vehicles influenced by lateral contact position, *Journal of Sound and Vibration* 267 (2003) 497–507.
[7] F.G. de Beer, M.H.A. Janssens, P.P. Kooijman, W.J. van Vliet, Curve squeal of railbound vehicles—part 1: frequency domain calculation model, Vol. 3, *Proceedings of Internoise*, Nice, France, 2000, pp. 1560–1563.
[8] P.P. Kooijman, W.J. van Vliet, M.H.A. Janssens, F.G. de Beer, Curve squeal of railbound vehicles—part 2: set-up for measurement of creepage dependent friction coefficient, Vol. 3, *Proceedings of Internoise*, Nice, France, 2000, pp. 1564–1567.
[9] M.H.A. Janssens, P.P. Kooijman, W.J. van Vliet, F.G. de Beer, Curve squeal of railbound vehicles—part 3: measurement method and results, Vol. 3, *Proceedings of Internoise*, Nice, France, 2000, pp. 1568–1571.
[10] A.H. Wickens, *Fundamentals of Rail Vehicle Dynamics: Guidance and Stability*, Swets & Zeitlinger, Lisse, 2003.
[11] J.J. Kalker, *Three Dimensional Bodies in Rolling Contact*, Kluwer Academic Publishers, Dordrecht, 1990.
[12] Z.Y. Shen, J.K. Hedrick, J.A. Elkins, A comparison of alternative creep-force models for rail vehicle dynamic analysis, *Proceedings of the Eighth IAVSD Symposium*, Cambridge, MA, Swets and Zeitlinger, Lisse, 1983, pp. 591–605.
[13] J.K. Hedrick, D.N. Wormley et al., Non-linear analysis and design tools for rail vehicles. Non-linear Locomotive Dynamics, AAR Report R-463, 1980.
[14] K. Kraft, Der Einfluss der Fahrgeschwindigkeit auf den Haftwert zwischen Rad und Schiene, *Archiv für Eisenbahntechnik* 22 (1967) 58–78.
[15] I.W. Kragelski, *Reibung und Verschliess*, VEB Verlag Technik, Berlin, 1971.